D″ beneath the Arctic from inversion of shear waveforms

Kenji Kawai,[1] Robert J. Geller,[2] and Nobuaki Fuji[2]

K. Kawai, Department of Earth and Planetary Sciences, Tokyo Institute of Technology, Ookayama 2-12-1, Meguro-ku, Tokyo, 152-8551, Japan. (kenji@geo.titech.ac.jp)

R.J. Geller and N. Fuji, Department of Earth and Planetary Science, Graduate School of Science, Tokyo University, Hongo 7-3-1, Bunkyo-ku, Tokyo, 113-0033, Japan. ([bob,fuji]@eps.s.u-tokyo.ac.jp)

[1]Department of Earth and Planetary Sciences, Tokyo Institute of Technology, Tokyo, Japan.

[2]Department of Earth and Planetary Science, Graduate School of Science, Tokyo University, Tokyo, Japan.

The structure of the D″ region beneath the Arctic has not previously been studied in detail. Using waveform inversion, we find that the average S-wave velocity in D″ beneath the Arctic is about 0.04 km/s higher than PREM, which is consistent with the existence of post-perovskite (ppv) in D″. It is difficult to strongly constrain the fine structure of S-velocity within D″ due to the small number of stations at epicentral distances $\Delta < 90°$, but by weighting those stations heavily in the inversion, we show that the data suggest the existence of high S-velocity in the upper half of D″ and low S-velocity in the lower half, consistent with the possibility of a double crossing (ppv $\rightarrow$ pv reverse phase transition) within D″. We conduct a computational experiment to show that resolution of the velocity structure within D″ could be significantly improved by temporary installation of a portable array of seismographs in northern Canada, which would greatly increase the number of stations in the range $70° < \Delta < 90°$.

1. Introduction

The lowermost 200-300 km of the mantle, which is known as the D″ layer, plays a crucial role in the Earth's deep interior. D″ has long been of great interest in geodynamics and mineral physics. Recent high-pressure experimental studies [see review by *Hirose,* 2006] have determined the pressure-temperature relations for many minerals. *Murakami et al.* [2004] found a phase transition (perovskite = pv → post-perovskite = ppv) at roughly the P-T conditions corresponding to the top of D″. *Hernlund et al.* [2005] suggested that, due to the extremely high temperature gradient near the core-mantle boundary (CMB), there should be a double crossing (reverse phase transition from ppv back to pv) within D″. *Kawai et al.* [2007], hereafter cited as KTGF07, used waveform inversion to study D″ beneath Central America and found evidence for high S-velocity in the upper half of D″ (which could correspond to ppv) and low S-velocity in the lower half of D″ (which could correspond to pv).

Due to the geometry of sources (deep or intermediate earthquakes) and receivers, D″ can only be studied beneath regions which are sampled by available event-receiver pairs. Fig. 1a shows the areas for which the S-velocity in D″ have been studied by previous works. In each case only the most recent paper for each area is shown. For some other areas the depth of D″ but not the S-velocity in D″ has been determined. These areas are not shown in Fig. 1a.

Previous studies analysed the velocity and the amplitude of Sd as a function of frequency and distance to obtain models of D″ [e.g., *Doornbos and Mondt,* 1979]. Although much previous work has been conducted using profiles of Sd for individual earthquakes [see

review by *Valenzuela and Wysession,* 1998], this is the first study which uses Sd waveforms of many stations for many events to systematically invert for the structure of D″. However, we show below that long-period Sd data are useful for determining the average S velocity in D″, but do not constrain the fine structure of S-velocity within D″. As we show below, detailed resolution on the fine structure of D″ is obtained from stations at epicentral distances $70° < \Delta < 90°$, i.e., from non-diffracted S-waves.

2. Target region and waveform data

We study the D″ layer beneath the Arctic Sea (Fig. 1a). The distribution of intermediate-depth earthquakes beneath the Hindu-Kush region and of receivers in North America, including the US-array, gives a large number of stations (Fig. 1b), almost all of which are at epicentral distances $\Delta > 90°$. Only eight stations are at $70° < \Delta < 90°$. In addition to the actual stations, Fig. 1b also shows a hypothetical network of possible stations in Western Canada at $70° < \Delta < 90°$. We discuss below the improvement in resolution of D″ that could be obtained if data from such a hypothetical network were available.

We use the transverse and radial components of broadband waveform data (obtained by rotating the N-S and E-W components) for 7 events (Table 1; Fig. 1b) from the IRIS/USGS, Transportable Array, ANZA, Nevada Regional Seismic Network, SCSN, PNSN, BDSN, and CNSN. We apply a bandpass filter to the data and construct datasets for the passband 0.005 to 0.05 Hz (i.e., for the period range, 20-200 s). In this study we use earthquakes which are sufficiently small that the source time function can be approximated as a δ-function at the centroid time for the frequency band used in the data

analysis. Our inverse formulation allows inversion for 3-D structure with all 21 elastic coeffients as unknowns [*Geller and Hara,* 1993]. However, due to the limited availability of data and various other uncertainties there are practical limitations on resolution. Because the dataset used in this study is small, we invert for a laterally homogeneous isotropic model.

We select time windows which include the first arrivals from the transverse component records and deconvolve the instrument response. We use the same selection criteria as KTGF07. The dataset consists of 202 time windows which satisfy the various criteria; 990 time windows which did not satisfy the criteria were rejected. The S/N ratio of the dataset is less than that of the dataset used by KTGF07, since the magnitude of the events used in this study is smaller and the diffracted waves used in this study have low amplitudes due to anelastic attenuation. We classify the waveform data into four groups based on their epicentral distances; Groups 1-4 are respectively from 70° to 80°, from 80° to 90°, from 90° to 100°, and greater than 100°. The number of time windows in each group is 11, 13, 136, and 142, respectively.

Since the inversion is only for the structure of D″ in the target region, other effects must be accounted for empirically. To correct for the effect of local structure near the stations and the sources, we make 'static' corrections using the time shift which gives the best correlation coefficient between the synthetic and observed seismograms. For $\Delta < 90°$, we use the arrivals of direct S waves as a reference (see KTGF07 for details). On the other hand, when the direct S wave also samples D″, S waves cannot be used as the reference. For $\Delta > 90°$, this study therefore uses SKS phases as the reference. This

method is similar to differential travel time analysis, which removes the effects of source- and receiver- structure using Sd and SKS phases which have approximately the same ray paths except for the target region [*Garnero and Helmberger,* 1993; *Kuo and Wu,* 1997]. As both SKS as well as Sd sample D″, the correction is not perfect. However, as the Sd phases sample D″ along a much longer path than SKS, we assume that the error can be neglected. Unlike the ScS-S pairs used in our previous study, the Sd-SKS pairs use phases from two orthogonal components (radial and transverse), which means that there is a possibility of errors due to anisotropy.

3. Inversion results

Our basic methodology follows KTGF07. The initial model is anisotropic PREM [*Dziewonski and Anderson,* 1981]. The source parameters (moment tensors and centroids) are fixed to the Harvard CMT solution. The S-wave velocities within 200 km of the CMB are the unknown parameters, while the S-velocities at shallower depths are fixed to PREM. We have not attempted to invert for the depth of D″, as that would require the use of shorter period waveform data. Our methods [*Geller and Hara,* 1993] are formulated to allow inversion for anisotropic elastic structure, but the present dataset has insufficient resolution to perform such an inversion.

We conduct inversions using the eigenvectors corresponding to the n largest eigenvalues of the singular value decomposition (SVD) of the matrix of partial derivatives (Fig. 2) as the basis functions for the perturbation to the starting model. We begin by using the reciprocal of the maximum amplitude in each time window as the weighting factor in the inversion, so that all data windows have roughly the same importance, and by using only

one eigenvector ($n = 1$) as the basis function, since the largest eigenvalue is much larger than the others. We call the resulting model SVD1NW (Fig. 3). The dataset used in this study is less sensitive to the depth-dependence of the S-velocity in D″ than the dataset used by KTGF07, although the amount of data is almost the same. As shown in Fig. 3 the unweighted inversion of long-period (periods of 20-200 s) diffracted shear waves can only resolve the average velocity structure in D″.

Table 2 shows the variance data. Defining the variance of the data to be 100 %, the variance of the synthetics for the initial model (PREM) is 319.5 %. This is reduced to 288.3 % when the time shift correction is applied. The residual for the model obtained by the above inversion (SVD1NW) is further reduced to 254.0 %. The variance in this study is much larger than that of KTGF07. This is because the dataset used in this study consists mainly of diffracted waves which are not only sensitive to the anelastic structure but are also very noisy. The variance is greater than 100% primarily because of the amplitude differences between the observed data and synthetics. However, despite the large variance, a meaningful value for the average shear velocity in D″ is obtained by the inversion. In the future the variance can probably be greatly reduced by performing waveform inversion for Q structure throughout the mantle.

Next we conduct another inversion in which data from stations at epicentral distances of $70^\circ < \Delta < 90^\circ$ (Groups 1 and 2) is emphasized. We use the reciprocal of the maximum amplitude in each window multiplied by factors of 40, 10, 1/20 and 1/30 as the respective weighting factors for Groups 1 to 4. We then conduct inversions using the eigenvectors corresponding to the n largest eigenvalues of the SVD as the basis functions for the

perturbations to the starting model obtaining models SVD1 and SVD2 for $n = 1$ and $n = 2$ respectively (Fig. 3). Table 2 shows variance data. In this case, the variance of the time-shifted data is dramatically smaller than the unshifted data for the initial model (PREM). SVD2 gives a large negative velocity gradient in D″ (Fig. 3). As shown by Table 2, the improvement in variance reduction for SVD1 vs. PREM with time shift is 0.4%, while the improvement in variance reduction for SVD2 vs. PREM with time shift is 2.1%. However (details omitted) further increasing the number of eignevalues does not yield a significant further variance reduction, so we choose SVD2 as the most appropriate model. For purposes of comparison, Fig. 3 also shows the models obtained using only one eignvector.

As shown in Fig. 3, SVD2 has high velocities in the upper half of D″ and low velocities in the lower half. In view of the relatively small number of data, this model cannot be regarded as quantitatively definitive, but this trend is likely to be real. Note that the average increase (relative to PREM) of S-velocities in D″ is 0.039 km/s for SVD1NW and 0.046 km/s for SVD2; i.e., roughly comparable values are obtained.

We conduct resolution tests in order to validate the inversion. All of the synthetic inversions can resolve a constant perturbation (Fig. 4a) although the amplitude of the perturbation is not fully recovered. SVD1NW and SVD2 can resolve the input model particularly well. Therefore, the average perturbation in D″, obtained by the actual inversions 0.03-0.04 km/s can be considered relatively reliable. The two-layered input model is successfully resolved by an inversion using two eigenvectors SVD2 (Fig. 4b). However, the number of time-windows in the range $70° < \Delta < 90°$ in the inversion is

very small – only twenty-four. Although the uncertainty is therefore large, the resolution test suggests that the spatial pattern of high and low velocities obtained by the actual inversion can be considered qualitatively reliable. However, in order to better constrain the internal structure of D″, more waveform data from stations in the range $70^\circ < \Delta < 90^\circ$ are required.

In order to investigate fine structure in D″ beneath the Arctic, we suggest that a temporary array network in Canada be deployed as shown in Fig. 1b. Here, we conduct a resolution test using the virtual stations (Figs. 2 and 4). In VS'SVD2 the synthetic virtual stations as well as the actual stations at $70^\circ < \Delta < 90^\circ$ are weighted by the same factors as we used for the actual stations in the inversion for SVD2. The synthetic tests show that the availability of data from the virtual stations would significantly enhance the resolution within D″ whether or not weighting is used. The actual deployment of a temporary array network in Canada would thus contribute greatly to investigation of the fine structure of D″ beneath the Arctic Sea.

4. Discussion

Murakami et al. [2007] reported that the shear velocity increase due to the pv → ppv phase transition is 0.5 to 1 % if ppv is isotropic. Thus the average velocity increase of 0.04 km/s in D″ found by our inversions may be interpreted as due to the phase transition from pv to ppv. If the gradient within D″ found in model SVD2 is correct, this may be interpreted as evidence for a double-crossing. KTGF07 found evidence for a double-crossing under Central America. Further evidence from other regions is needed, to determine the extent to which that the double-crossing is a global phenomenon.

Acknowledgments. We thank Kei Hirose for valuable discussions. Data were provided by the BDSN, CNSN, and IRIS data centers. We also thank two anonymous reviewers for valuable comments. This research was partly supported by grants from the Japanese Ministry of Education, Science and Culture (Nos. 17540392 and 19740272).

References

Avants, M., T. Lay, S.A. Russell, and E.J. Garnero (2006), Shear velocity variation within the D″ region beneath the central Pacific, *J. Geophys. Res.*, *111*, B05305, doi:10.1029/2004JB003270.

Doornbos, D.J., and J.C. Mondt (1979), P and S waves diffracted around the core and the velocity structure at the base of the mantle, *Geophys. J. R. Astr. Soc.*, *57,* 381–395.

Dziewonski, A.M., and D.L. Anderson (1981), Preliminary reference Earth model, *Phys. Earth Planet. Inter.*, *25,* 297–356.

Ford, S.R., E.J. Garnero, and A.K. McNamara (2005), A strong lateral shear velocity gradient and anisotropy heterogeneity in the lowermost mantle beneath the southern Pacific, *J. Geophys. Res.*, *111,* B03306, doi:10.1029/2004JB003574.

Fouch, M.J., K.M. Fischer, and M.E. Wysession (2001), Lowermost mantle anisotropy beneath the Pacific: Imaging the source of the Hawaiian plume, *Earth Planet. Sci. Lett.*, *190,* 167–180.

Garnero, E.J, and D.V. Helmberger (1993), Travel times of S and SKS: Implications for three-dimensional lower mantle structure beneath the Central Pacific, *J. Geophys. Res.*, *98,* 8225–8241.

Geller, R.J., and T. Hara (1993), Two efficient algorithms for iterative linearized inversion of seismic waveform data, *Geophys. J. Int.*, *115,* 699–710.

Hernlund, J.W., C. Thomas, and P.J. Tackley (2005), A doubling of the post-perovskite phase boundary and structure of the Earth's lowermost mantle, *Nature*, *434,* 882–886.

Hirose, K. (2006), Postperovskite phase transition and its geophysical implications, *Rev. Geophys.*, *44,* RG3001, doi:10.1029/2005RG000186.

Kawai, K., N. Takeuchi, R.J. Geller, and N. Fuji (2007), Possible evidence for a double crossing phase transition in D″ beneath Central America from inversion of seismic waveforms, *Geophys. Res. Lett.*, *34,* L09314, doi:10.1029/2007GL029642.

Kito, T., F. Kruger, and H. Negishi (2004), Seismic heterogeneous structure in the lowermost mantle beneath the southwestern Pacific, *J. Geophys. Res.*, *109,* B09304, doi:10.1029/2003JB002677.

Kuo, B.Y., and K.Y. Wu (1997), Global shear velocity heterogeneities in the D″ layer: Inversion from *Sd-SKS* differential travel times, *J. Geophys. Res.*, *102,* 11775–11788.

Moore, M.M., E.J. Garnero, T. Lay, and Q. Williams (2004), Shear wave splitting and waveform complexity for lowermost mantle structures with low-velocity lamellae and transverse isotropy, *J. Geophys. Res.*, *109,* B02319, doi:10.1029/2003JB002546.

Murakami, M., K. Hirose, K. Kawamura, N. Sata, and Y. Ohishi (2004), Post-perovskite phase transition in $MgSiO_3$, *Science*, *304,* 855–858.

Murakami, M, S.V. Sinogeikin, J.D. Bass, N. Sata, Y. Ohishi, and K. Hirose (2007), Sound velocity of $MgSiO_3$ post-perovskite phase: A constraint on the D″ discontinuity, *Earth Planet. Sci. Lett., 259,* 18–23.

Ni, S., D.V. Helmberger, and J. Tromp (2005), Three-dimensional structure of the African superplume from waveform modelling, *Geophys. J. Int.*, *161,* 283–294.

Ritsema, J. (2000), Evidence for shear velocity anisotropy in the lowermost mantle beneath the Indian Ocean, *Geophys. Res. Lett.*, *27,* 1041–1043.

Thomas, C., J.-M. Kendall, and J. Lowmann (2004), Lower mantle seismic discontinuities and the thermal morphology of subducted slabs, *Earth Planet. Sci., Lett.*, *225*, 105–113.

Usui, Y., Y. Hiramatsu, M. Furumoto, and M. Kanao (2005), Thick and anisotropic D″ layer beneath Antarctic Ocean, *Geophys. Res. Lett.*, *32,* L13311, doi:10.1029/2005GL022622.

Valenzuela, R.W., and M.E. Wysession (1998), Illuminating the base of the mantle with diffracted waves, in *The Core-Mantle Boundary Region, Geodyn. Ser.*, Vol. 28, edited by M. Gurnis, et al., pp. 57–71, AGU, Washington, D.C.

Event #	Date (Y/M/D)	Latitude	Longitude	Depth	M_w
1	2000/5/1	37.82°	72.43°	152.0	5.6
2	2001/2/25	36.41°	70.62°	193.4	6.1
3	2004/4/5	36.52°	70.84°	183.5	6.5
4	2004/8/10	36.52°	70.60°	205.7	6.0
5	2005/7/23	36.40°	70.65°	212.9	5.5
6	2005/12/12	36.45°	71.06°	210.2	6.5
7	2007/4/3	36.57°	70.59°	221.4	6.2

Table 1. Earthquakes used in this study.

	Model	variance %	$\delta\beta$ km/s
(I)	PREM	319.5	-
	PREM with time shift	288.3	-
	SVD1NW	254.0	0.039
(II)	PREM	240.5	-
	PREM with time shift	157.0	-
	SVD1	156.6	0.016
	SVD2	154.9	0.046

Table 2. Variance and average perturbation to shear velocity in D″ for each model. (I) Inversion using the reciprocal of the maximum amplitude in each time window as the weighting factor. (II) Inversion heavily weighting the waveforms at epicentral distances between 70° and 90° (see text for details).

Figure 1. (a) Global map centered around the north pole showing regions for which the velocities within the D″ layer have been studied. Only the most recent study for each region is shown. (b) Event-receiver geometry, with great circle ray paths. The portions of the great circles which sample D″ are shown in red. Reversed triangles, circles, and squares show the sites of North American stations (data from IRIS/USGS, Transportable Array, ANZA, Nevada Regional Seismic Network, SCSN, PNSN, BDSN, and CNSN) used in our study, and colors indicate the groups to which the stations belong. Red stars show the seven intermediate depth earthquakes studied. Purple diamonds show the twenty virtual stations.

Figure 2. The first ten eigenvalues of the SVD, with the largest eigenvalue normalized to one. We also show the eigenvalues for a hypothetical dataset including the virtual stations in Fig. 1b. The weighting factor for the virtual stations is the same as was used for the actual stations in the weighted and unweighted inversions. n is the order number of the sorted eigenvalues, where $\lambda_1 > \lambda_2 \cdots$.

Figure 3. Results of the SVD inversions for uniform weighting (SVD1NW) and for heavy weighting of the waveforms in the range $70^\circ < \Delta < 90^\circ$ (SVD1 and SVD2). See text for details.

Figure 4. Synthetic resolution test for D″ structure. All inversions can successfully resolve a constant velocity perturbation. Inversions heavily weighting the waveforms in the range $70^\circ < \Delta < 90^\circ$ (SVD2) can qualitatively resolve the two-layered model (b). With the virtual stations, the two-layered model can be well-resolved with or without variable weighting.

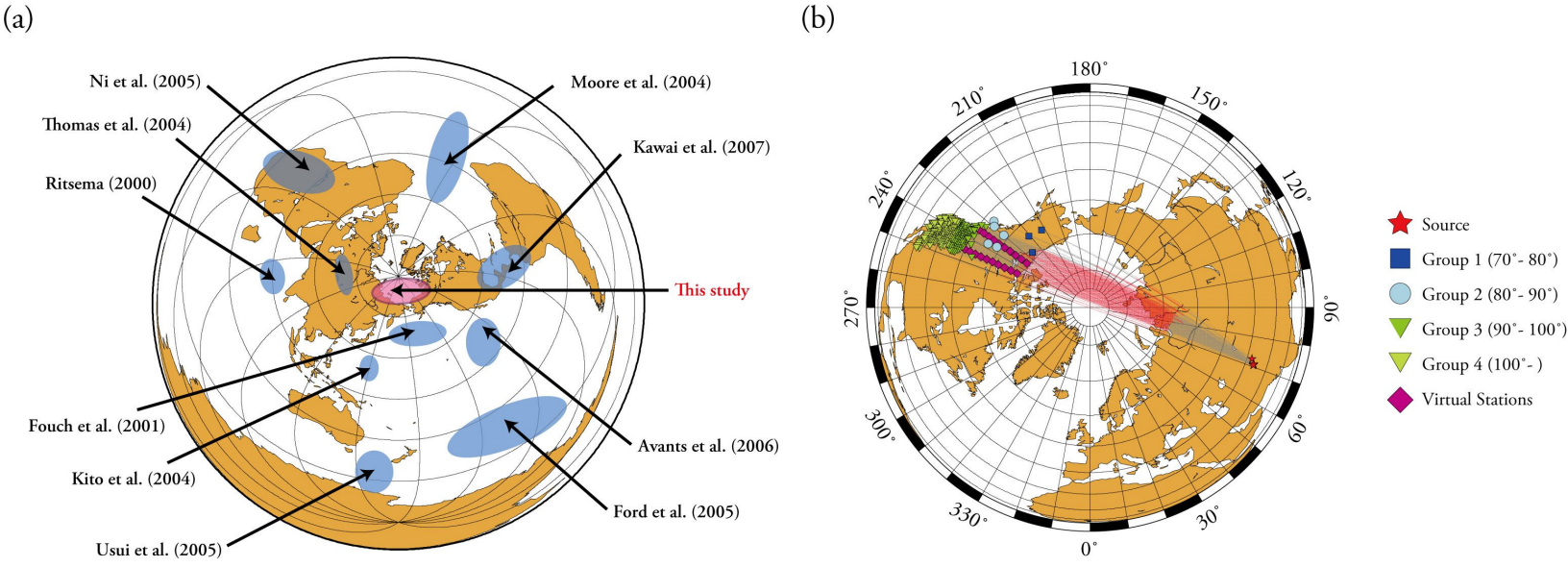

Kawai et al. Fig.1

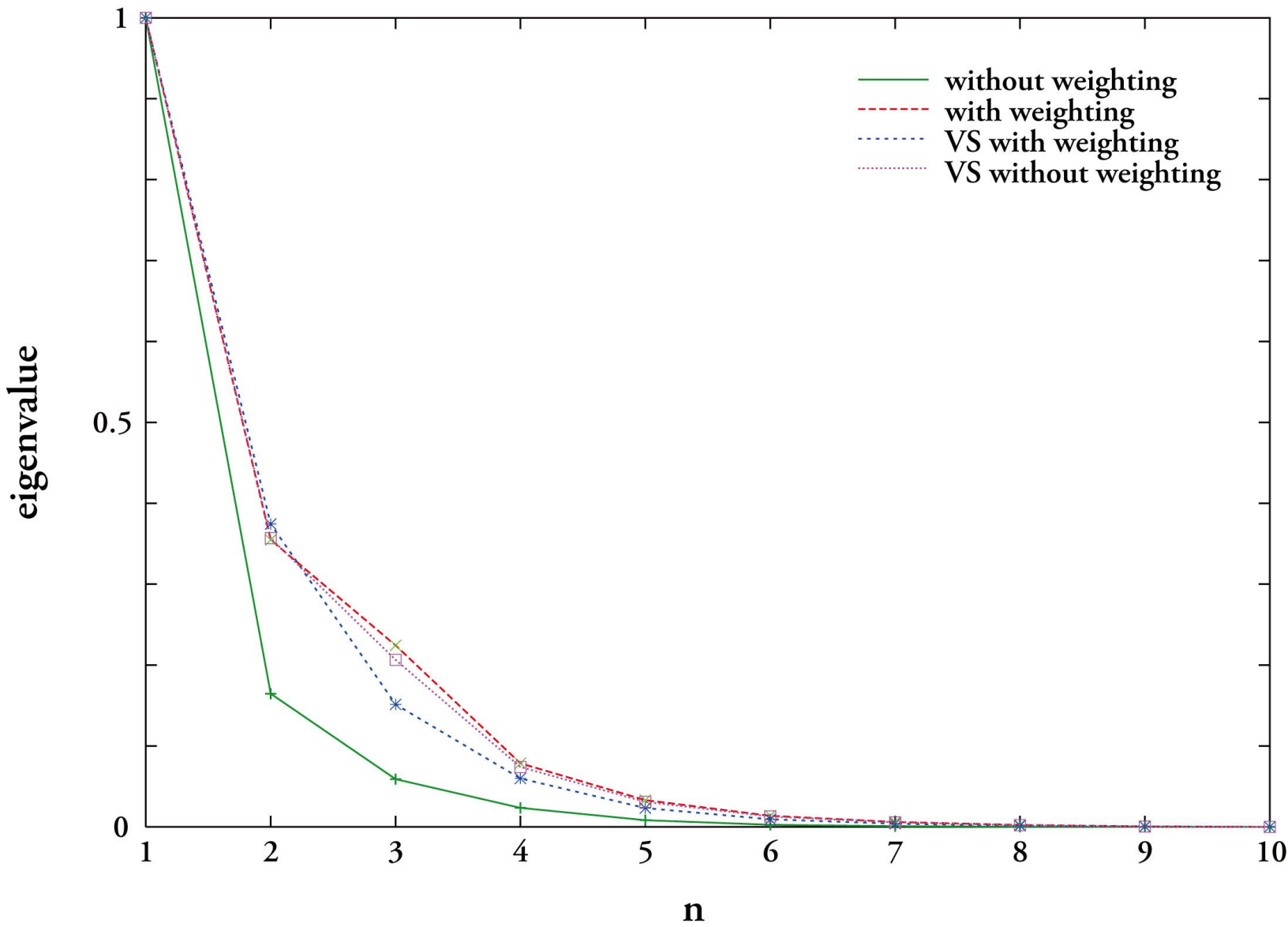

Kawai et al. Fig. 2

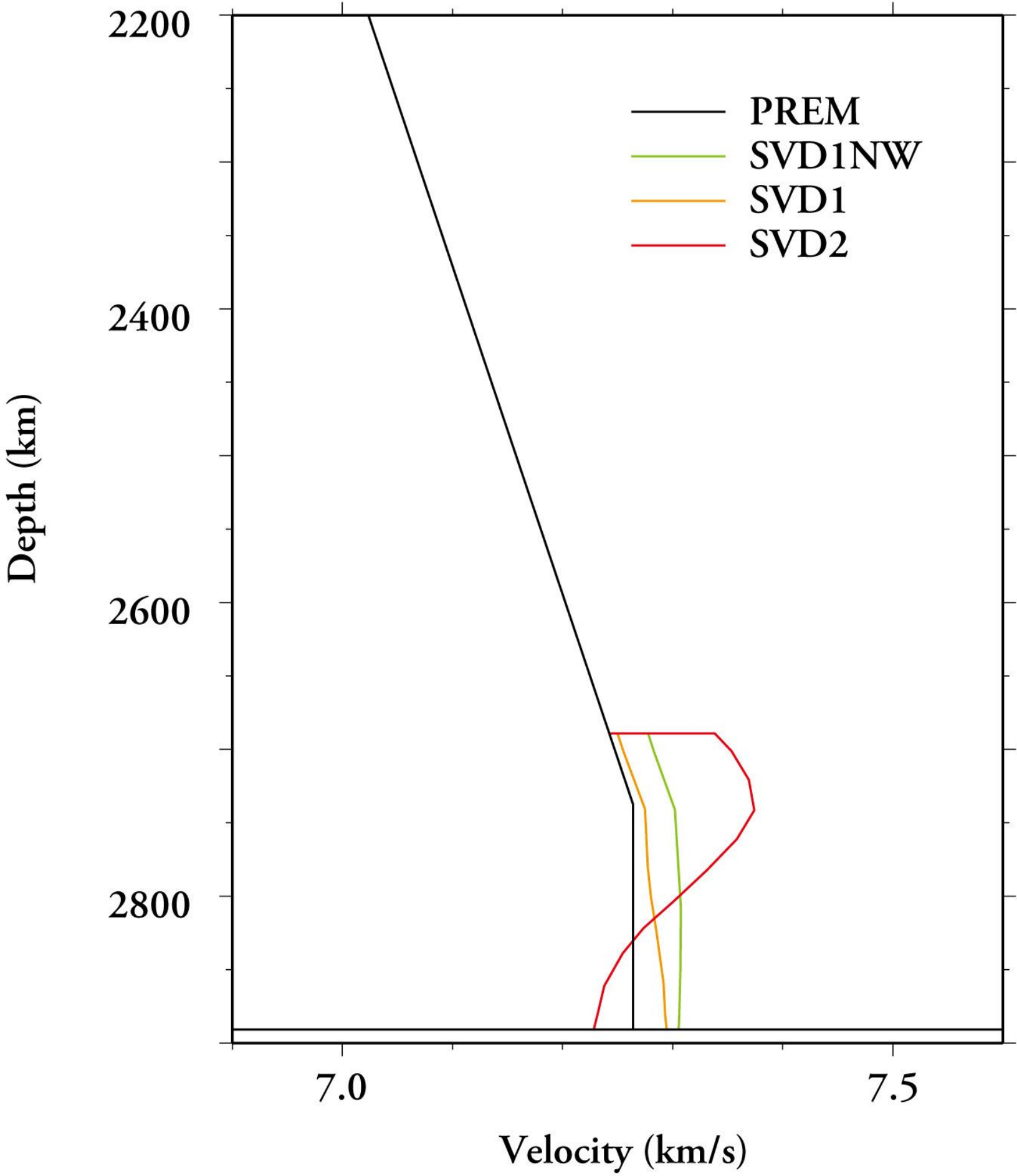

Kawai et al. Fig. 3

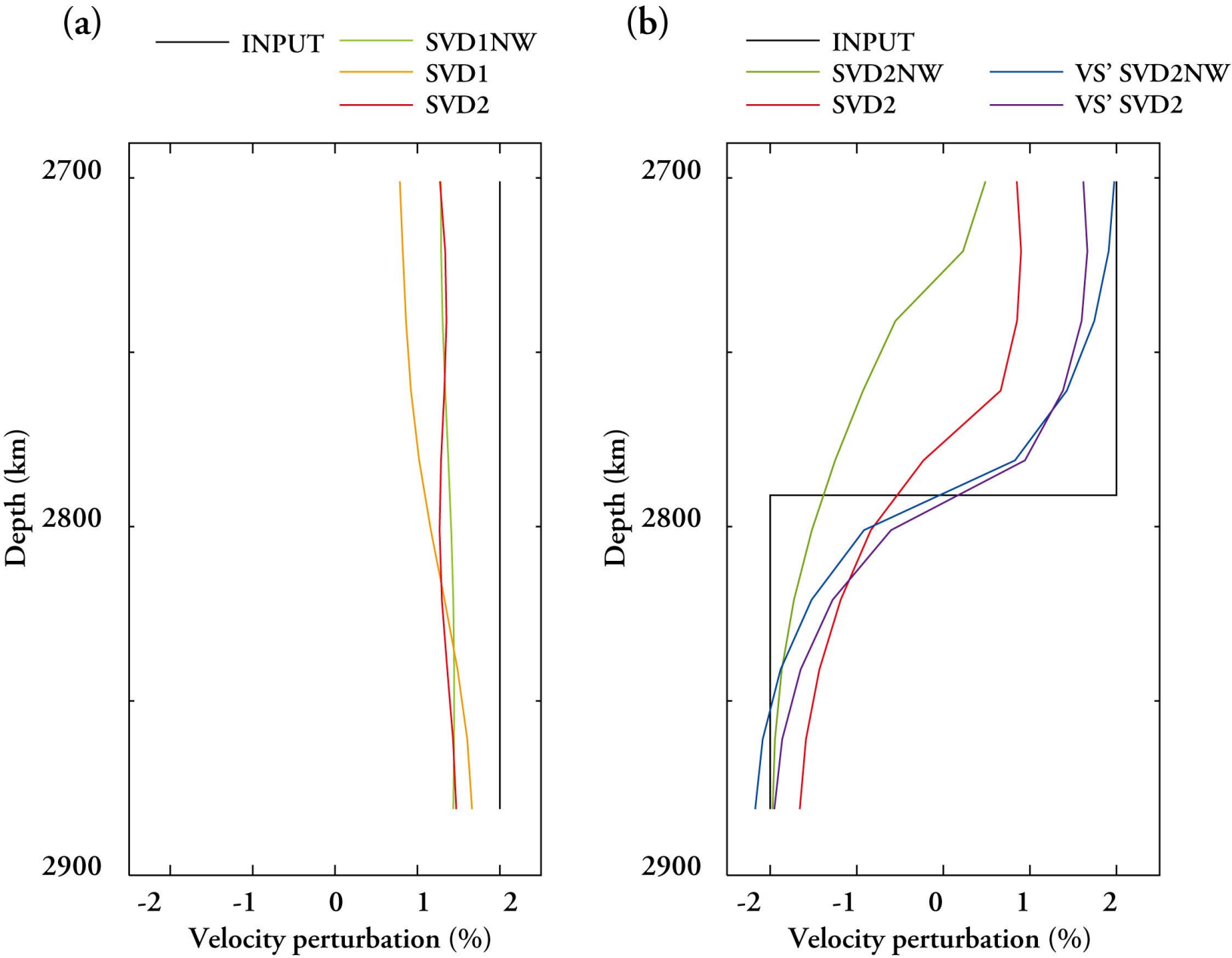

Kawai et al. Fig. 4